



## TECHNICAL NOTE

# DEPENDENCE OF THE CHARGE TRANSFER SPECTRA OF $(\text{C}_2\text{H}_5\text{NH}_3)_2\text{CdCl}_4 : \text{Cu}^{2+}$ WITH HYDROSTATIC PRESSURE: STRUCTURAL CHANGES AROUND $\text{Cu}^{2+}$

B. AMAYA MORAL and FERNANDO RODRIGUEZ

Departamento CITIMAC, Facultad de Ciencias, Universidad de Cantabria, 39005 Santander, Spain

(Received 23 April 1996; accepted 7 January 1997)

**Abstract**—This paper investigates the variation of the charge transfer (CT) spectra of the  $\text{Cu}^{2+}$  doped  $(\text{EtNH}_3)_2\text{CdCl}_4$  ( $\text{Et} = \text{C}_2\text{H}_5$ ) layer perovskite under hydrostatic pressure. The aim is to explain the strong redshift ( $\sim 4000 \text{ cm}^{-1}$ ) undergone by the first CT band of the formed  $\text{CuCl}_6^{4-}$  complex on passing from  $(\text{EtNH}_3)_2\text{CdCl}_4 : \text{Cu}^{2+}$  to the isomorphous  $(\text{EtNH}_3)_2\text{MnCl}_4 : \text{Cu}^{2+}$  crystal, which is accompanied by a change of color from light yellow to deep red. The pressure experiments show that the first  $\text{Cl}^- \rightarrow \text{Cu}^{2+}$  CT band experience an abrupt shift of  $\sim 1200 \text{ cm}^{-1}$  between 23 and 26 kbar. The comparison of these results with those previously obtained in the pure  $(\text{EtNH}_3)_2\text{CuCl}_4$  suggests that this shift is associated with a local change around the  $\text{Cu}^{2+}$  from an elongated octahedron geometry ( $P = 1 \text{ atm}$ ) to a more compressed situation similar to that found for the Mn crystal. © 1997 Elsevier Science Ltd. All rights reserved

## 1. INTRODUCTION

The optical properties of halide compounds doped with the Jahn-Teller  $\text{Cu}^{2+}$  ion ( $d^9$  configuration) strongly depend upon the local geometry around the impurity and its ligands  $\text{CuX}_n$  ( $n = 4, 6$ ) complex. The occurrence of a given geometry is mainly determined by the coordination number and crystal anisotropy, thus a great variety of structures can be found in  $\text{Cu}^{2+}$  doped materials depending on the crystallographic structure and composition of the host crystal. In the case of  $\text{CuCl}_6^{2-}$  complexes, different local geometries have been observed between the square planar ( $D_{4h}$ ) and the tetrahedral ( $T_d$ ) symmetries, most of the complexes have bending distortions of  $D_{2d}$  symmetry with  $\text{Cl}-\text{Cu}-\text{Cl}$  angles ranging from  $124$  to  $180^\circ$  [1]. For  $\text{CuX}_6^{4-}$  complexes, the situation is more complicated since the coordination geometry can vary from the elongated tetragonal to the compressed one ( $D_{4h}$ ), through different orthorhombic intermediates ( $D_{2h}$ ) [2]. The elongated fluoride  $\text{CuF}_6^{4-}$  complexes ( $D_{4h}$ ) found in  $\text{CuF}_2$  and  $\text{Na}_2\text{CuF}_4$  [3] and the compressed ones ( $D_{4h}$ ) found in  $\text{KCuAlF}_6$  [4],  $\text{Ba}_2\text{ZnF}_6 : \text{Cu}^{2+}$  [5] and  $\text{K}_2\text{ZnF}_4 : \text{Cu}^{2+}$  [6, 7] are examples of this behavior.

In chlorides, the usual local structure observed in  $\text{CuCl}_6^{4-}$  corresponds to the elongated situation nearly  $D_{4h}$  in  $\text{CdCl}_2 : \text{Cu}^{2+}$  [8],  $\text{LiCl} : \text{Cu}^{2+}$  [9],  $(\text{EtNH}_3)_2\text{CuCl}_4$  [10] or orthorhombic  $D_{2h}$  in  $(\text{EtNH}_3)_2\text{CdCl}_4 : \text{Cu}^{2+}$  [11],  $(\text{CH}_3)_4\text{NCdCl}_3 : \text{Cu}^{2+}$  [12] and in mixed crystals of (3-chloroanilinium) $_8[\text{Cd}_{1-x}\text{Cu}_x\text{Cl}_6]\text{Cl}_4$  [2, 13–15]. Exceptions to this behavior have been found first in

$(\text{enH}_2)\text{MnCl}_4 : \text{Cu}^{2+}$  [16] and later in the  $\text{A}_2\text{MnCl}_4 : \text{Cu}^{2+}$  ( $\text{A} = \text{C}_n\text{H}_{2n+1}\text{NH}_3$  with  $n = 1, 2$ ) [11] layered perovskites where a  $D_{4h}$  compressed geometry has been proposed for explaining to the broad absorption band at  $21\,000 \text{ cm}^{-1}$  (476 nm) [16, 17] which is responsible for the intense red color exhibited by these crystals. The existence of such compressed geometry was argued in terms of crystal anisotropy at the Mn site in these layer perovskites. In fact, the  $\text{A}_2\text{MCl}_4$  ( $\text{M} = \text{Mn, Fe, Cd}$ ) crystals are ideal systems for accommodating substitutional cations in nearly  $D_{4h}$  compressed sites. In this structure, the  $\text{MCl}_6$  units form layers by sharing each of the four equatorial Cl ligands with the four nearest neighbor cations as is shown in Fig. 1. The shortest  $\text{M}-\text{Cl}$  bonds in  $\text{MCl}_6$  correspond to terminal Cl ligands and are perpendicular to the layer ( $c$  direction). The equatorial and axial  $\text{M}-\text{Cl}$  distances are  $R_{\text{eq}} = 2.67 \text{ \AA}$  and  $R_{\text{ax}} = 2.52 \text{ \AA}$  for  $(\text{EtNH}_3)_2\text{CdCl}_4$  [18] while for  $(\text{EtNH}_3)_2\text{MnCl}_4$  the distances are  $R_{\text{eq}} = 2.59 \text{ \AA}$  and  $R_{\text{ax}} = 2.47 \text{ \AA}$  [19].

Nevertheless the optical properties of  $\text{A}_2\text{CdCl}_4 : \text{Cu}^{2+}$  [11] and  $\text{A}_2\text{MnCl}_4 : \text{Cu}^{2+}$  [11, 16] which are governed by the  $\text{Cl}^- \rightarrow \text{Cu}^{2+}$  charge transfer (CT) bands of the formed  $\text{CuCl}_6^{4-}$  complex are very different despite the resemblance shown by the Cd and Mn sites in their respective crystals. In particular, the color of these doped crystals is light yellow in  $\text{A}_2\text{CdCl}_4 : \text{Cu}^{2+}$  and deep red in  $\text{A}_2\text{MnCl}_4 : \text{Cu}^{2+}$ . Recent investigations carried out in the mixed crystals  $\text{A}_2\text{Mn}_{1-x}\text{Cd}_x\text{Cl}_4 : \text{Cu}_{2+}$  [11] clearly show that the local geometry around  $\text{Cu}^{2+}$  in  $\text{A}_2\text{CdCl}_4 : \text{Cu}^{2+}$  ( $x = 1$ ) is

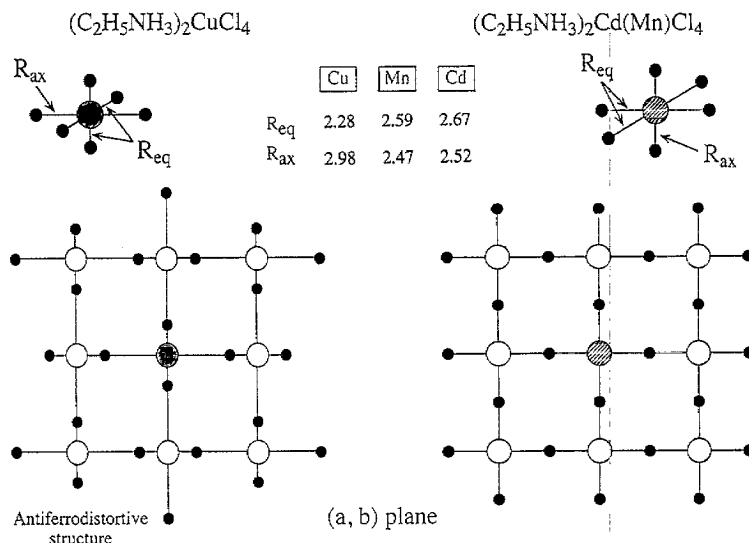


Fig. 1. Schematic view of the (001) basal plane of the  $(C_2H_5NH_3)_2MCl_4$  layer perovskite ( $M = Cu$  (left) and  $M = Cd, Mn$  (right)). Note the antiferrodistortive structure displayed by the  $CuCl_6^{4-}$  units in  $(C_2H_5NH_3)_2CuCl_4$ . In both structures the terminal Cl ligands are placed above and below the M cation. An schematic view of the  $MCl_6$  unit is depicted above the corresponding a-b plane. Bond lengths,  $R_{eq}$  and  $R_{ax}$ , are given in Å.

elongated  $D_{2h}$  (nearly  $D_{4h}$ ) instead of being compressed. The long axial Cu-Cl bond and one of the short equatorial Cu-Cl bonds lie on the (001) basal plane, and are randomly distributed between the two possible orthogonal directions, resembling the antiferrodistortive structure displayed by the  $Cu^{2+}$  complexes in the pure  $A_2CuCl_4$  crystals [20] (Fig. 1).

The aim of the present work is to investigate the variation of the CT spectra of  $(EtNH_3)_2CdCl_4: Cu^{2+}$  with hydrostatic pressure using a sapphire anvil cell. This method enables to reduce the cell volume of the  $(EtNH_3)_2CdCl_4: Cu^{2+}$  crystal thus approaching the structural situation attained in  $(EtNH_3)_2MnCl_4: Cu^{2+}$ . Although hydrostatic pressure techniques have been widely employed to investigate the effects of pressure on the spectra and geometry changes of  $Cu^{2+}$  complexes [20–22], this is the first work dealing with pressure effects on  $Cu^{2+}$  doped perovskites through CT spectroscopy. Interestingly, the variety of colors exhibited by these layer perovskites doped with  $Cu^{2+}$  makes them useful as potential candidates for piezochromism.

## 2. EXPERIMENTAL

Single crystals of  $(EtNH_3)_2CdCl_4$  and  $(EtNH_3)_2MnCl_4$  doped with  $Cu^{2+}$  (0.1 mol %) were grown from slow evaporation as described elsewhere [11]. The room temperature orthorhombic structure (*Amba* space group) was checked by X ray diffraction. Several microcrystal c-plates were selected for optical studies under hydrostatic pressure. Crystal dimensions were about  $100 \times 100 \times 20 \mu m^3$ .

The optical spectra were recorded with a double beam

spectrometer specially designed for hydrostatic pressure cells [24]. A sapphire anvil cell was used for this purpose [24, 25]. Paraffin oil was used as pressure transmitter. The pressure was calibrated through the luminescence of a small ruby chip placed near the sample. The pressure was determined from the redshift of the R lines by the equation  $P(kbar) = 27.5 \Delta\lambda(nm)$ . The ruby was excited with the 568 nm beam of a coherent I-302-K krypton laser.

## 3. SPECTROSCOPIC MEASUREMENTS: ANALYSIS AND DISCUSSION

Fig. 2 shows the optical absorption (OA) spectra of the  $(EtNH_3)_2CdCl_4: Cu^{2+}$  and  $(EtNH_3)_2MnCl_4: Cu^{2+}$  crystals at room temperature. The two bands at 25 100 and 35 600  $cm^{-1}$  (398 and 281 nm, respectively) observed in the Cd crystal, are assigned to  $Cl^- \rightarrow Cu^{2+}$  CT transitions. Within an elongated  $D_{4h}$  symmetry framework for  $CuCl_6^{4-}$ , these correspond to electronic transitions from the mainly bonding  $Cl^- e_u(\pi + \sigma)$  and  $e_u(\sigma + \pi)$  molecular orbitals (MO) to the antibonding mainly  $Cu^{2+} b_{1g}(x^2 - y^2)$  MO, respectively, according to previous analysis given elsewhere [11]. On the other hand, the presence of a new band at 21 000  $cm^{-1}$  in the Mn perovskite is characteristic of compressed octahedral  $CuCl_6^{4-}$  units [16, 17].

Fig. 3 shows the evolution of the first CT band of  $(EtNH_3)_2CdCl_4: Cu^{2+}$  with pressure up to 31 kbar. The corresponding variation of the peak energy of the first CT band versus pressure is plotted in Fig. 4. As regards to the spectra, two important facts can be noticed: (i) The absorption band at 25 100  $cm^{-1}$  (398 nm) experiences a

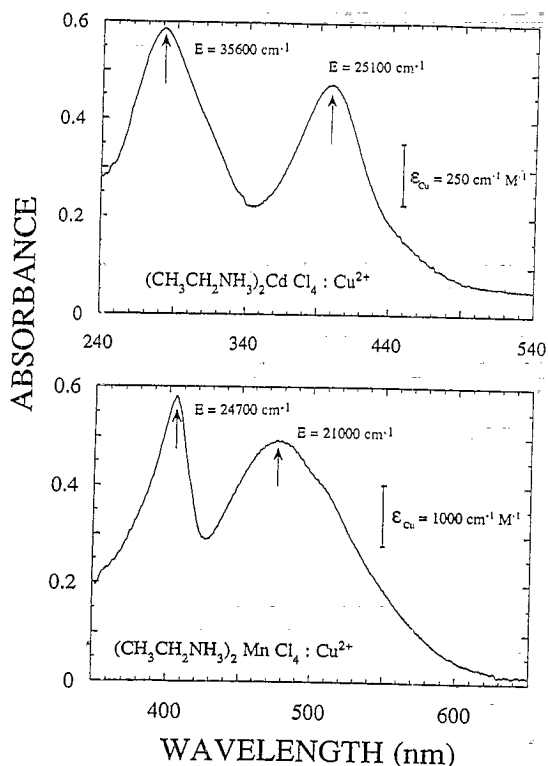


Fig. 2. Optical absorption spectra corresponding to isomorphous microcrystals of  $(\text{C}_2\text{H}_5\text{NH}_3)_2\text{CdCl}_4 : \text{Cu}^{2+}$  and  $(\text{C}_2\text{H}_5\text{NH}_3)_2\text{MnCl}_4 : \text{Cu}^{2+}$  at atmospheric pressure.

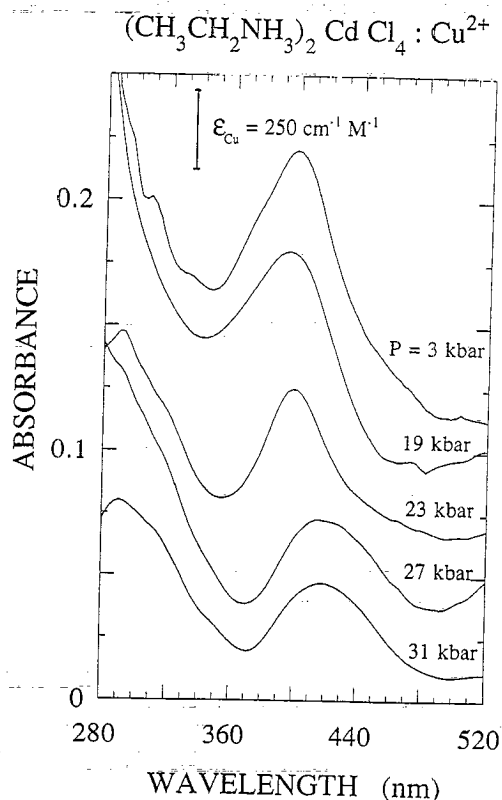


Fig. 3. Variation of the first CT band of  $(\text{C}_2\text{H}_5\text{NH}_3)_2\text{CdCl}_4 : \text{Cu}^{2+}$  with pressure up to 31 kbar. Note the strong variation experienced by the first CT band above 23 kbar. For comparison, a constant absorption background was added to each spectrum.

small redshift from atmospheric pressure to 23 kbar at a rate of  $-4 \text{ cm}^{-1}/\text{kbar}$ . (ii) Above this pressure, the CT band abruptly shifts by  $-1400 \text{ cm}^{-1}$  to lower energies. This strong variation reflects a change of the local structure of  $\text{Cu}^{2+}$  induced by pressure. Pressure-induced structural changes in  $\text{CuCl}_4^{2-}$  complexes have been widely investigated in many pure compounds such as  $(\text{R}_n\text{NH}_{4-n})_2\text{CuCl}_4$  ( $\text{R} = \text{alkyl}$ ;  $n = 1-4$ ) [23] and  $\text{Cs}_2\text{CuCl}_4$  [21, 22], some of which show thermochromism associated with structural changes around  $\text{Cu}^{2+}$  at phase transitions. The effect of increasing pressure, or also decreasing temperature in the thermochromics, is mainly to stabilize the square-planar geometry ( $\text{D}_{4h}$ ) with respect to the tetrahedral distorted geometry ( $\text{D}_{2d}$ ) [23].

For  $\text{CuCl}_6^{4-}$ , though much less investigated than  $\text{CuCl}_4^{2-}$ , the comparison of the present results with those obtained in the pure  $(\text{EtNH}_3)_2\text{CuCl}_4$  crystal [26] allows us to ascribe the CT redshift observed above 23 kbar to a structural change of the  $\text{CuCl}_6^{4-}$  complex from the elongated octahedron to a more compressed situation. This change can be described in such way that the effect of pressure upon the complex is mainly to reduce the in-plane longest axial Cu-Cl bond length and probably to increase the in-plane equatorial distance, leading to a more compressed situation with the shortest axial Cu-Cl bond now associated with the terminal ligand along  $c$ . The interpretation can explain the

observed redshift according to what would be expected on the basis of the results  $(\text{EtNH}_3)_2\text{MnCl}_4 : \text{Cu}^{2+}$  [11, 16, 17]. Furthermore, the hydrostatic pressure experiments performed by Moritomo and Tokura [26] on  $(\text{EtNH}_3)_2\text{CuCl}_4$  support the present interpretation. A strong redshift of  $-2400 \text{ cm}^{-1}$  is observed in the pure crystal with increasing pressure up to 40 kbar. This shift is also

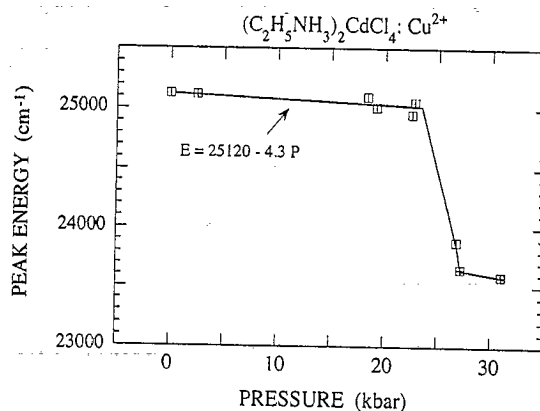


Fig. 4. Variation of the peak energy of the first CT band of  $(\text{C}_2\text{H}_5\text{NH}_3)_2\text{CdCl}_4 : \text{Cu}^{2+}$  with pressure. The abrupt jump of  $-1400 \text{ cm}^{-1}$  takes place above 23 kbar. Between atmospheric pressure and 23 kbar, the peak energy is linear with pressure at a rate of  $-4 \text{ cm}^{-1}/\text{kbar}$ .

accompanied by the deactivation of the Raman peaks which are associated with vibrations of the in-plane  $\text{Cl}^-$  ligands, thus indicating the progressive disappearance of the antiferrodistortive structure upon pressure, i.e. the axial and the equatorial Cu–Cl bond distances approach each other upon pressure [26]. However, further investigations using diffraction techniques at high pressures are required in order to confirm this interpretation as well as to clarify whether the abrupt CT redshift in  $(\text{EtNH}_3)_2\text{CdCl}_4$ :  $\text{Cu}^{2+}$  is just a pure local phenomenon or whether it is associated with a phase transition of the host crystal, driving the structural change around the  $\text{Cu}^{2+}$ . In either case, the results of the present work indicate that the pressure-induced redshift observed in  $(\text{EtNH}_3)_2\text{CuCl}_4$  seems to be connected to structural changes of the  $\text{CuCl}_6^{4-}$  unit rather than to a broadening of the interband transition as suggested in Ref. [26]. The observations of this behavior in diluted systems rules out this latter possibility.

The present results are in agreement with findings in the mixed the  $\text{A}_2\text{Cd}_{1-x}\text{Mn}_x\text{Cl}_4$ :  $\text{Cu}^{2+}$  crystal series [11, 27] (chemical pressure). However, an important enhancement of the  $\text{Cu}^{2+}$  molar extinction coefficient,  $\epsilon_{\text{Cu}}$ , was observed upon increasing the  $\text{Mn}^{2+}$  concentration ( $x$ ). This enhancement of CT intensity was ascribed to exchange effects between  $\text{Cu}^{2+}$  and its four nearest  $\text{Mn}^{2+}$  whose excited crystal field states are resonant with the  $\text{Cl}^- \rightarrow \text{Cu}^{2+}$  CT states of  $\text{CuCl}_6^{4-}$  [27].

**Acknowledgements**—Fernando Rodriguez is indebted to Prof. H.U. Güdel for introducing him to the field of hydrostatic pressure techniques during his stay at the University of Bern and the collaboration in this field. We thank R. Valiente and B. Baticle for assistance in the crystal growing and structural characterization. Financial support from Caja Cantabria, the Vicerrectorado de Investigación of the University of Cantabria and the CICYT (Project No PB92-0505) is acknowledged.

## REFERENCES

1. Marco de Lucas, M.C., Rodriguez, F. and Aramburu, J.A., *J. Phys.: Condens. Matter*, 1991, **3**, 8945 and references quoted therein.
2. Hitchman, M.A., *Comm. Inorg. Chem.*, 1994, **15**, 197.
3. Oelkrug, D., *Structure and Bonding*, 1971, **9**, 1.
4. Finnie, K., Dubicki, L., Krausz, E.R. and Riley, M.J., *Inorg. Chem.*, 1990, **29**, 3908.
5. Reinen, D., Steffen, G., Hitchman, M.A., Strateimer, H., Dubicki, L., Krausz, E.R., Riley, M.J., Mathies, H.E., Recker, K. and Wallrafen, F., *Chem. Phys.*, 1991, **155**, 117.
6. Riley, M.J., Hitchman, M.A. and Reinen, D., *Chem. Phys.*, 1986, **102**, 11.
7. Riley, M.J., Dubicki, L., Moran, G., Krausz, E.R. and Yamada, I., *Chem. Phys.*, 1990, **145**, 363.
8. Kan'no, K., Naoe, S., Mukai, S. and Nakai, Y., *Solid State Commun.*, 1973, **13**, 1325.
9. Hirako, S. and Onaka, R., *J. Phys. Soc. Jpn*, 1982, **51**, 1255.
10. Desjardins, S.R., Penfield, K.W., Cohen, S.L., Musselman, R.L. and Solomon, E.I., *J. Am. Chem. Soc.*, 1983, **105**, 4590.
11. Baticle, B., Rodriguez, F. and Valiente, R., *Rad. Eff. & Def. Sol.*, 1995, **135**, 587.
12. Valiente, R., Marco de Lucas, M.C. and Rodriguez, F., *J. Phys.: Condens. Matter*, 1995, **7**, 3881.
13. Tucker, D., White, P.S., Trjan, K.L., Kirk, M.L. and Hatfield, W.E., *Inorg. Chem.*, 1991, **30**, 823.
14. Ellis, P.J., Freeman, H.C., Hitchman, M.A., Reinen, D. and Wagner, B., *Inorg. Chem.*, 1994, **33**, 1249.
15. Burkhard, W., Warda, S.A., Hitchman, M.A. and Reinen, D., *Inorg. Chem.*, 1996, **35**, 3967.
16. Schmid, U., Güdel, H.U. and Willet, R.D., *Inorg. Chem.*, 1982, **21**, 2977.
17. Aramburu, J.A. and Moreno, M., *J. Chimie Physique*, 1989, **86**, 871.
18. Chapuis, G., *Phys. Stat. Sol. A*, 1977, **43**, 203.
19. Depmeier, W., *Acta Cryst. B*, 1976, **32**, 303.
20. Steadmen, P.J. and Willet, R.D., *Inorg. Chim. Acta*, 1970, **4**, 367.
21. Wang, P.J. and Drickamer, H.G., *J. Chem. Phys.*, 1973, **59**, 559.
22. Bray, K.L. and Drickamer, H.G., *J. Phys. Chem.*, 1990, **94**, 2154.
23. Ferraro, J.R., *Vibrational Spectroscopy at High External Pressures. The Diamond Anvil Cell*, Chapter 5 and the references therein. Academic Press, London, 1984.
24. Moral, B.A. and Rodriguez, F., *Rev. Sci. Inst.*, 1995, **66**, 5178.
25. Riesen, H., Kindler, U. and Güdel, H.U., *Rev. Sci. Inst.*, 1987, **58**, 1122.
26. Moritomo, Y. and Tokura, Y., *J. Chem. Phys.*, 1994, **101**, 1763.
27. Valiente, R. and Rodriguez, F., *J. Phys. Chem. Solids*, 1996, **57**, 571.